

Abstract

Experiments involving boron incorporation into brucite ($\text{Mg}(\text{OH})_2$) from magnesium-free artificial seawater with pH values ranging from 9.5 to 13.0 were carried out to better understand the incorporation behavior of boron into brucite. The results show that both concentration of boron in deposited brucite ($[\text{B}]_d$) and its boron partition coefficient (K_d) between deposited brucite and final seawater are controlled by pH of the solution. The incorporation capacity of boron into brucite is much stronger than that into oxides and clay minerals. The isotopic compositions of boron in deposited brucite ($\delta^{11}\text{B}_d$) are higher than those in the associated artificial seawater ($\delta^{11}\text{B}_{\text{isw}}$) with fractionation factors ranging between 1.0177 and 1.0569, resulting from the preferential incorporation of $\text{B}(\text{OH})_3$ into brucite. Both boron adsorptions onto brucite and precipitation reaction of H_3BO_3 with brucite exist during deposition of brucite from artificial seawater. The simultaneous occurrence of both processes determines the boron concentration and isotopic fractionation of brucite. The isotopic fractionation behaviors and mechanisms of boron incorporated into brucite are different from those into carbonates. Furthermore, the isotopic compositions of boron in modern corals might be affected by the existence of brucite in madrepore and the preferential incorporation of $\text{B}(\text{OH})_3$ into brucite. An exploratory study for the influence of brucite on the boron isotopic composition in modern corals is justifiable.

1 Introduction

Mg is a common trace element in the *scleractinian* corals and Mg/Ca ratio has been used to investigate paleothermometry of seawater (Watanabe et al., 2001; Marshall and McCulloch, 2002; Mitsuguchi et al., 2008; Allison et al., 2010). Mg can exist in the form of brucite in corals (Smith and Delong, 1978; Nothdurft et al., 2005) and Mg content in *scleractinian* corals varies between different genera and localities (Fallon et al., 1999). Nothdurft et al. (2005) studied brucite in living *scleractinian* corals colonies

CPD

7, 887–920, 2011

Boron isotope fractionation during brucite deposition

J. Xiao et al.

Title Page

Abstract

Introduction

Conclusions

References

Tables

Figures

◀

▶

◀

▶

Back

Close

Full Screen / Esc

Printer-friendly Version

Interactive Discussion



(*Acropora*, *Pocillopora*, *Porites*) from subtidal and intertidal settings in the Great Barrier Reef, Australia, and subtidal *Montastraea* from the Florida Keys, United States. Their results suggested that high containing activity combined with high pH and low $p\text{CO}_2$ led to localized brucite precipitation in organic biofilms of coral skeletons and that brucite in living coral skeletons is an indicator of extreme microenvironments in shallow-marine settings. The occurrence of brucite in corals could be responsible for reported anomalies in Mg/Ca vs. sea-surface temperature (SST) plots in corals (Nothdurft et al., 2005). However, little attention has been paid to the influence of brucite on the boron isotopic composition of corals.

Studies of boron isotopic compositions of minerals have been developed (Palmer and Swihart, 1996; Pokrovsky and Schott, 2004; Pokrovsky et al., 2005; Sanchez-Valle et al., 2005). In minerals as clay and other layered hydroxides, surface charge properties play an important role by changing the apparent acid-base equilibrium constant (Sanchez-Valle et al., 2005). Boric acid can inhibit the dissolution of brucite (Pokrovsky et al., 2005) and the tendency of adsorbing boron onto brucite or hydrous ferric oxide (HFO) is relatively strong (Petric et al., 1998; Wang, 2003; Liu et al., 2004). Peak et al. (2003) investigated the mechanism of boric acid ($\text{B}(\text{OH})_3$) and borate ($\text{B}(\text{OH})_4^-$) adsorption onto HFO, suggesting that $\text{B}(\text{OH})_3$ may be the main species adsorbed onto HFO. Liu et al. (2004) studied the mechanism of boron absorption by brucite, suggesting that the adsorption was controlled by solution pH and only the $\text{B}(\text{OH})_4^-$ species was absorbed onto the brucite surface. However, the influence of brucite on boron isotopic fractionation during adsorption is not researched, so that the mechanism of boron incorporated into brucite is unclear.

In recent years, topics such as the reconstruction of ancient seawater pH using the isotopic composition of boron in bio-carbonates, the calculation of the past $p\text{CO}_2$, and the influence of these two factors on changes in the ancient climate, have become important issues for the international boron isotope geochemistry community (Vengosh et al., 1991; Hemming and Hanson, 1992, 1995; Spivack et al., 1993; Gaillardet and Allègre, 1995; Sanyal et al., 1995, 1997; Palmer et al., 1998; Pearson and Palmer,

Boron isotope fractionation during brucite deposition

J. Xiao et al.

Title Page

Abstract

Introduction

Conclusions

References

Tables

Figures



Back

Close

Full Screen / Esc

Printer-friendly Version

Interactive Discussion



Boron isotope fractionation during brucite deposition

J. Xiao et al.

Title Page

Abstract

Introduction

Conclusions

References

Tables

Figures



Back

Close

Full Screen / Esc

Printer-friendly Version

Interactive Discussion



1999, 2000; Lécuyer et al., 2002; Hönisch and Hemming, 2005; Hönisch et al., 2008). Whether the $\delta^{11}\text{B}$ of bio-carbonate is equal to that of $\text{B}(\text{OH})_4^-$, and what the theoretic fractionation factor (α_{4-3}) between $\text{B}(\text{OH})_4^-$ and $\text{B}(\text{OH})_3$ is, have emerged as the main questions involved in these issues. A series of inorganic calcite precipitation experiments have shown that $\text{B}(\text{OH})_4^-$ is the dominant species incorporated into calcite (Palmer et al., 1987; Hemming et al., 1995; Sanyal et al., 1996, 2000). However, Klochko et al. (2009) recently found that both trigonal and tetrahedral coordinated boron existed in biogenic and hydrothermal carbonates. Inorganic calcite precipitation experiment has been carried out by Xiao et al. (2006), indicating that the $\delta^{11}\text{B}$ of inorganic calcium carbonate did not in parallel with the calculated curve of $\text{B}(\text{OH})_4^-$, but deviated increasingly from the parallel trend as pH increased. When pH was increased to a certain value, the isotopic fractionation factor of boron between precipitation and solution was greater than 1. Xiao et al. (2006) reasoned that the presence of Mg^{2+} or other microelements was the main reasons of this observation and concluded that $\text{B}(\text{OH})_3$ may incorporate preferentially into brucite. If this is true, the isotopic compositions of boron in modern corals might be affected by the existence of brucite in madrepora and the preferential incorporation of $\text{B}(\text{OH})_3$ into brucite.

In this study, experiments on the incorporation of boron during the deposition of brucite from magnesium-free artificial seawater at various pH values were carried out. The incorporation species of boron into brucite and the boron isotope fractionation during deposition of brucite were discussed. This result will shed some light on the application of boron isotope-paleo-pH proxy in corals.

2 Methods

2.1 Reagents and equipment

1.0 M HCl, 0.5 M NaOH, and 0.5 M MgCl_2 were prepared using boron-free water with twice distilled HCl (GR), NaOH (GR), and MgCl_2 (GR), respectively. The concentration

Boron isotope fractionation during brucite deposition

J. Xiao et al.

Title Page

Abstract

Introduction

Conclusions

References

Tables

Figures

⏪

⏩

◀

▶

Back

Close

Full Screen / Esc

Printer-friendly Version

Interactive Discussion



each beaker to achieve the following range of pH values: 9.50, 10.00, 10.50, 11.00, 11.50, 12.00, 12.50, and 13.00. 8 mL of MgCl_2 solution was then added dropwise into the artificial seawater with different pH values. During this process, NaOH was added to keep the pH at the predetermined pH values as the brucite was deposited. The pH fluctuations were measured by a pH meter with a precision of 0.01. A magnetic stirrer was used during the experiments process to ensure the reactions were completed. The experiment was terminated after 8 mL of MgCl_2 was added. After mixing well the deposit and solution, the mixture was divided into two parts evenly. One was encountered filtration by pumping immediately to isolate deposit from solution (defined as a repose time $T_r = 0$ h) and the other was encountered filtration by pumping after reposing for 20 h (defined as a repose time $T_r = 20$ h). The separated solution was placed in air-tight plastic bottles, and the brucite deposit was washed with boron-free water until Cl^- was no longer detected. Then the deposited material was dried at 60°C and placed in air-tight plastic bottles.

2.4 Separation of boron from the samples

In preparation for isotopic measurement, boron was extracted from the artificial seawater and the brucite using a two-step chromatographic technique (Wang et al., 2002). About 0.5 mL of Amberlite IRA 743 boron-specific resin with 80–100 mesh was placed in a polyethylene column with a diameter of 0.2 cm. The length of the resin bed was 1.5 cm. About 200 mg of brucite was first dissolved using a slightly excessive amount of boron-free HCl solution, passed through a column filled with Amberlite IRA 743 resin, and then eluted using approximately 5 mL of 0.1 M HCl at 75°C . An amount of mannitol approximately equimolar to the boron content was added to the eluate, which was then desiccated to near dryness by partial evaporation in a super clean oven with laminar flow at 60°C (Xiao et al., 2003). The solution was then loaded again into the column filled with a mixed resin composed of 0.5 mL cation-exchange resin (H^+ form) and 0.5 mL anion-exchange resin (ion-exchange II, HCO_3^- form). The boron was eluted by 5 mL of boron-free water. The eluate was evaporated again at 60°C to produce a

solution with a boron concentration of about 1 µg B/µL for isotopic measurement. The procedures for extracting boron in the liquid samples were the same as those described above. The total boron blank in chemical process and filament loading was determined by isotope dilution mass spectrometry (IDMS) to contain 46 ng of boron.

5 2.5 Measurements of boron concentration and isotopic composition

The boron concentrations were determined by the azomethine-H spectrophotometric method. One mL of sample solution, 2 mL of buffer solution, and 2 mL of azomethine-H solution were added in that order. After thorough mixing, each solution was allowed to stand for 120 min. The absorption of the boron-azomethine-H complex was measured at 420 nm using a spectrophotometer. The external precision of the azomethine-H method used here was 2%.

The isotopic compositions of boron in all samples were measured by a GV Iso-Probe T single magnetic sector thermal ionization mass spectrometer and the P-TIMS method using Cs_2BO_2^+ ions with a graphite loading (Xiao et al., 1988). Two µL of graphite slurry was first loaded onto a degassed tantalum filament, and then approximately 1 µL of sample solution containing about 1–4 µg of boron and an equimolar amount of mannitol were also loaded. This was followed by 1–2 µL of a Cs_2CO_3 solution containing an equimolar amount of cesium. The loaded material was dried by heating the filament at 1.2 A for 5 min.

The data were collected by switching the magnetic field between the masses 308 ($^{133}\text{Cs}_2^{10}\text{B}^{16}\text{O}_2^+$) and 309 ($^{133}\text{Cs}_2^{11}\text{B}^{16}\text{O}_2^+$), and the intensity ratios of the ion beams at masses 308 and 309 ($R_{309/308}$) were calculated. Calibrated with oxygen isotopes, the $^{11}\text{B}/^{10}\text{B}$ ratio was calculated as $R_{309/308} - 0.00078$. The isotopic composition of boron was expressed as an $\delta^{11}\text{B}$ value according to the following formula:

$$\delta^{11}\text{B}(\text{‰}) = \left[\left(\frac{^{11}\text{B}/^{10}\text{B}}{\text{sample}} \right) / \left(\frac{^{11}\text{B}/^{10}\text{B}}{\text{standard}} \right) - 1 \right] \times 1000$$

Boron isotope fractionation during brucite deposition

J. Xiao et al.

Title Page

Abstract

Introduction

Conclusions

References

Tables

Figures



Back

Close

Full Screen / Esc

Printer-friendly Version

Interactive Discussion



Here the standard material is NIST SRM 951, the recommended value of which is 4.04362 ± 0.00137 (Catanzaro et al., 1970). The measured average $^{11}\text{B}/^{10}\text{B}$ ratio of NIST SRM 951 was 4.0525 ± 0.0027 ($2\sigma_m$, $n = 5$).

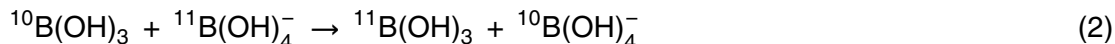
3 Results and discussion

3.1 Dissolved boron species and boron isotope in seawater

The dominant aqueous species of boron in seawater are $\text{B}(\text{OH})_3$ and $\text{B}(\text{OH})_4^-$. The relative proportions of these species are a function of pH (Fig. 1a) and given by the following relation:



Figure 1 shows the theoretical distribution of boron species as a function of pH for seawater. At low pH ($\text{pH} < 7$), virtually all of the boron in seawater is in the $\text{B}(\text{OH})_3$ species; conversely, at high pH ($\text{pH} > 10$), virtually all of the boron is in the $\text{B}(\text{OH})_4^-$ species (Fig. 1a). The isotope exchange reaction between these species is given by:



The distribution of species and the isotope exchange reaction are solved simultaneously to give the isotopic composition of the individual boron species vs. pH for seawater (Fig. 1b). The abundances of two stable isotopes ^{11}B and ^{10}B at pH 8 make up approximately 80% and 20% of the total boron, respectively. Modern seawater has a boron concentration of about 4.5 ppm, and a consistent, worldwide $\delta^{11}\text{B}$ isotopic composition of +39.5‰ relative to NIST SRM 975. Only the $\text{B}(\text{OH})_4^-$ incorporated into the marine bio-carbonates is one of the essential hypotheses for using boron isotopic composition in marine bio-carbonate to reconstruct the paleo-environment.

Boron isotope fractionation during brucite deposition

J. Xiao et al.

Title Page

Abstract

Introduction

Conclusions

References

Tables

Figures

◀

▶

◀

▶

Back

Close

Full Screen / Esc

Printer-friendly Version

Interactive Discussion



3.2 The partition coefficient of boron between Brucite and final seawater

The boron concentrations and the partition coefficients (K_d) between brucite and final seawater are listed in Table 2, and shown in Fig. 2. The results are showed as follows:

1. The variation trend of the results for $T_r = 0$ h and $T_r = 20$ h are basically the same (Fig. 2a), indicating the incorporation of boron into brucite deposit is instantaneous, and the reaction time is not a main limiting factor. This finding is consistent with the previous study (Liu et al., 2004).
2. When pH is lower than 10, $[B]_{\text{fsw}}$ decreases as the pH increases, and reaches the lowest value at pH 10 (Fig. 2a). This indicates that the amount of boron incorporated into deposited brucite increases as pH increases, and reaches the highest value at pH 10. $[B]_{\text{fsw}}$ increases quickly at higher pH values, and no smooth trend is observed, indicating that the amount of incorporated boron decreases quickly.
3. When pH is lower than 10, K_d increases as the pH increases (Fig. 2b). The K_d reaches its highest values of 487.5 and 494.2 for $T_r = 0$ h and $T_r = 20$ h at pH 10, respectively. When pH is higher than 10, K_d decreases and shows a mild trend after pH 12.

The K_d between brucite deposit and final seawater can be shown as:

$$K_d = (f \times K_{d3} + K_{d4}) / (1 + f). \quad (3)$$

$$K_d = \{[B_3]_{\text{solid}} + [B_4]_{\text{solid}}\} / \{[B_3]_{\text{fluid}} + [B_4]_{\text{fluid}}\}, K_{d3} = [B_3]_{\text{solid}} / [B_3]_{\text{fluid}},$$

$K_{d4} = [B_4]_{\text{solid}} / [B_4]_{\text{fluid}}, f = [B_3]_{\text{fluid}} / [B_4]_{\text{fluid}}, K_{d3}$ and K_{d4} are the partition coefficient of $B(OH)_3$ and $B(OH)_4^-$, respectively. f_3 is the ratio of $B(OH)_3$ to $B(OH)_4^-$ in solution. This equation indicates that K_d is not only related with K_{d3} and K_{d4} , but also with the fraction of $B(OH)_3$ in solution. The K_d between clay minerals and seawater is 3.60 at $T = 5^\circ\text{C}$ and pH 8.45 (Palmer, 1987), but the highest K_d in our experiments is 494 at pH 10, which is much higher than 3.6. It indicates that the K_{d3} is much greater than

Boron isotope fractionation during brucite deposition

J. Xiao et al.

Title Page

Abstract

Introduction

Conclusions

References

Tables

Figures

◀

▶

◀

▶

Back

Close

Full Screen / Esc

Printer-friendly Version

Interactive Discussion



**Boron isotope
fractionation during
brucite deposition**

J. Xiao et al.

Title Page

Abstract

Introduction

Conclusions

References

Tables

Figures



Back

Close

Full Screen / Esc

Printer-friendly Version

Interactive Discussion



K_{d4} , i.e. the incorporation capacity of $B(OH)_3$ into brucite is much higher than that of $B(OH)_4^-$ and the K_{d3} contribution is dominating. The quantity of brucite reaches its highest at pH 10, indicating the reaction equivalence point of brucite deposition occurs approximately at pH 10. The K_d also reach its highest at pH 10. When pH is higher than 10, the f and K_{d3} decreases while K_{d4} increases as the increasing pH. Although the increasing concentration of OH^- in solution can influence the adsorption of $B(OH)_4^-$ (Keren et al., 1981), the adsorption of $B(OH)_4^-$ continues, and the K_{d4} still increases perhaps. Because of K_{d3} is greater than K_{d4} , the decreasing of K_{d3} is dominating, so that the K_d decreases with the increasing pH. In the studies of Xu and Ye (1997), the point of zero charge (PZC) of brucite is close to 11.9, which is approximates to the inflexion point (pH 12) in our experiment. When pH is higher than PZC, anions will not be adsorbed by goethite and gibbsite (Kingston et al., 1972), so that the adsorption ability of $B(OH)_4^-$ by brucite decreases greatly when pH is higher than the PZC of brucite. Therefore, K_d should monotonically decrease with increasing pH as well.

Boron removal experiments by magnesium hydroxide at different pH values have been carried out by Liu et al. (2004), Fuente and Muñoz (2006) and Yuan et al. (2006). They attributed the adsorption of $B(OH)_4^-$ to the magnesium hydroxide. Their results showed that $[B]_{fsw}$ reached its lowest values at pH 9.3 or 10, which indicates that adsorption had reached its highest values. The $[B]_{fsw}$ then increased slowly at higher pH values. The results of the present study are consistent with their works.

There is a slight difference in the variation of $[B]_d$ with pH for different T_r values. When $T_r = 0$ h and pH = 9.5, $[B]_d$ is slightly lower than that at pH 10, and the highest $[B]_d$ value of 937.8 ppm also appears at pH 10. But when $T_r = 20$ h, the maximum $[B]_d$ may appear at pH ≤ 9.5 , while the highest value at pH 9.5 is 1859 ppm, which is much higher than 951.5 ppm at pH 10. Considering the slight difference in the boron balance time of the deposited $Mg(OH)_2$, the value for $T_r = 20$ h may be more reliable.

The evolution pattern of boron incorporated into the $Mg(OH)_2$, and the variations in partition coefficients with pH, are basically the same as those of oxides and clay minerals. However, the maximum amounts of incorporated boron in brucite or other

hydroxides are much higher than those of the oxides and clay minerals (Keren et al., 1981, 1983; Goldberg and Glaubig, 1985, 1986; Lemarchand et al., 2005, 2007), indicating the incorporation capacity of boron on hydroxides is stronger than that on both oxides and clay minerals.

3.3 Isotopic fractionation of boron between deposited brucite and solution

Isotopic compositions of boron in deposited brucite ($\delta^{11}\text{B}_d$) and final seawater ($\delta^{11}\text{B}_{\text{fsw}}$) are listed in Table 3 and shown in Fig. 3. The crucial points illustrated in Fig. 3 are summarized as follows:

1. The variation trend of the results for $T_r = 0$ h and $T_r = 20$ h are basically same (Fig. 3a). This indicates that the isotopic balance between brucite deposit and solution is instantaneous, and that the results of the experiment are exact. A minor difference between $T_r = 0$ h and $T_r = 20$ h appears at the pH increases from 9.5 to 10.0. When $T_r = 0$ h, $\delta^{11}\text{B}_d$ and $\alpha_{d-\text{fsw}}$ both increase as the pH increases from 9.5 to 10.0. However, when $T_r = 20$ h, $\delta^{11}\text{B}_d$ and $\alpha_{d-\text{fsw}}$ both decrease as the pH increases from 9.5 to 10.0. This is perhaps related to the fact that the formation of brucite is slower in low pH than in high pH.
2. All the $\delta^{11}\text{B}_d$ values are enriched in the heavy isotope relative to the $\delta^{11}\text{B}_{\text{fsw}}$ (Fig. 3a). All the $\alpha_{d-\text{fsw}}$ are greater than 1 (Fig. 3b), which is entirely different from those of the carbonates deposits (Fig. 3c). As $\text{B}(\text{OH})_4^-$ is incorporated preferentially into carbonate deposits, all the $\delta^{11}\text{B}$ values of carbonates are lower than that of the parent seawater. Meanwhile, all the isotopic fractionation factors $\alpha_{\text{carb}-\text{sw}}$ between carbonates and seawater are lower than 1 and increase with pH. In this study, the $\alpha_{d-\text{fsw}}$ between brucite deposit and solution shows a waved pattern (Fig. 3b), suggesting a complex isotopic fractionation process.

The $\delta^{11}\text{B}_d$, $\delta^{11}\text{B}_{\text{ISW3}}$ and $\delta^{11}\text{B}_{\text{ISW4}}$ of $\text{B}(\text{OH})_3$ and $\text{B}(\text{OH})_4^-$ in initial seawater, calculated using the different α_{4-3} versus pH values of the parent solutions, are shown

Boron isotope fractionation during brucite deposition

J. Xiao et al.

Title Page

Abstract

Introduction

Conclusions

References

Tables

Figures

◀

▶

◀

▶

Back

Close

Full Screen / Esc

Printer-friendly Version

Interactive Discussion



Boron isotope fractionation during brucite deposition

J. Xiao et al.

Title Page

Abstract

Introduction

Conclusions

References

Tables

Figures

◀

▶

◀

▶

Back

Close

Full Screen / Esc

Printer-friendly Version

Interactive Discussion



in Fig. 4. When $T_r = 0$ h, the $\delta^{11}\text{B}_d$ values are equal to or lower than the $\delta^{11}\text{B}_{\text{isw3}}$ calculated using $\alpha_{4-3} = 0.9600$. When $T_r = 20$ h, the $\delta^{11}\text{B}_d$ values are equal to or lower than the $\delta^{11}\text{B}_{\text{isw3}}$ calculated using $\alpha_{4-3} = 0.9397$, but all the $\delta^{11}\text{B}_d$ values are higher than $\delta^{11}\text{B}_{\text{isw}}$ (Fig. 4). The α_{4-3} of 0.9600 and 0.9397 is calculated according to the highest $\delta^{11}\text{B}$ of deposited brucite for $T_r = 0$ h and $T_r = 20$ h. If $\delta^{11}\text{B}_d$ is equal to $\delta^{11}\text{B}_{\text{isw3}}$, it implies that only $\text{B}(\text{OH})_3$ is incorporated into $\text{Mg}(\text{OH})_2$, which is impossible under normal circumstances. Moreover a situation in which $\delta^{11}\text{B}_d > \delta^{11}\text{B}_{\text{isw3}}$ would be even more improbable. Except for pH 9.5, $\delta^{11}\text{B}_d$ values are lower than $\delta^{11}\text{B}_{\text{isw3}}$ calculated using $\alpha_{4-3} = 0.9600$ (Fig. 4), so that the true α_{4-3} would have to be lower than 0.9600, which is a little lower than the currently expected value between 0.983 and 0.952 (Zeebe, 2005). The pH values used in previous carbonates precipitation experiments are lower than 9.0, while that of our experiments are between 9.5 and 13.0. The differences of the experiments conditions may result diverse α_{4-3} , but which value is much more reliable or what is the true α_{4-3} is still uncertain. Our results also indicate that $\delta^{11}\text{B}_d$ is not parallel with $\delta^{11}\text{B}_{\text{isw3}}$, but first decreases and then increases with an inflexion at pH 12. All of the data indicate that both $\text{B}(\text{OH})_3$ and $\text{B}(\text{OH})_4^-$ are incorporated into the deposited brucite.

The fractions of $\text{B}(\text{OH})_3$ (F_{d3}) in the brucite deposit calculated using $\alpha_{4-3} = 0.9397$ and $\alpha_{4-3} = 0.9600$ are shown in Fig. 5. It seems that F_{d3} tends to decrease with decreasing α_{4-3} . Because the adopted α_{4-3} is not true, the calculated F_{d3} is not exact. The true F_{d3} could be lower than the value indicated in Fig. 5, but the variation trend of F_{d3} with pH should be certain and much higher than that of the initial artificial seawater (F_{isw3}). The $\delta^{11}\text{B}_d$ is the concurrent result of $\delta^{11}\text{B}_{d3}$ and $\delta^{11}\text{B}_{d4}$. Here $\delta^{11}\text{B}_d$ can be shown as:

$$\delta^{11}\text{B}_d = f_{d3} \times \delta^{11}\text{B}_{d3} + (1 - f_{d3}) \times \delta^{11}\text{B}_{d4} \quad (4)$$

Boron isotope fractionation during brucite deposition

J. Xiao et al.

Title Page

Abstract

Introduction

Conclusions

References

Tables

Figures



Back

Close

Full Screen / Esc

Printer-friendly Version

Interactive Discussion



where f_{d3} is the fraction of $B(OH)_3$ in solid. During pH 10–12, both $\delta^{11}B_{d3}$ and $\delta^{11}B_{d4}$ increases with increasing pH (Fig. 1b). Therefore, the $\delta^{11}B_d$ should be increased with the increasing pH, but the increasing trend is inconspicuous (Fig. 3a). There are two reasons accounting for this. On the one hand, the increasing $\delta^{11}B_{d3}$ and $\delta^{11}B_{d4}$ can result in the increasing of $\delta^{11}B_d$. On the other hand, with the increasing pH, the dominant decreasing incorporation fraction of $B(OH)_3$ and increasing incorporation fraction of $B(OH)_4^-$ will result the decreasing of $\delta^{11}B_d$. With the common influence of these two aspects, the variation of $\delta^{11}B_d$ with pH is small. When pH reaches 12 (PZC of brucite), the adsorption quantity of $B(OH)_4^-$ decreases suddenly, while that of $B(OH)_3$ increases (Fig. 5). So the $\delta^{11}B_d$ increases.

3. The manner in which α_{d-fsw} changes with pH for $T_r = 0$ h and 20 h is shown in Fig. 3b. Except for pH 9.5, both patterns are basically the same for each T_r , and match the change in F_{d3} shown in Fig. 5. The α_{d-fsw} values decrease as the pH increases from 9.5 to 12, and reach the lowest point at pH 12. Then α_{d-fsw} values increase rapidly. The α_{d-fsw} reflects the relative ratio of $B(OH)_3$ to $B(OH)_4^-$ in brucite.

The explanation of $\delta^{11}B_d$ with pH can be also used to the explanation of boron fractionation factor between brucite and solution. When pH from 10 to 12, incorporation fraction of $B(OH)_3$ decreases continuously (Fig. 5), and contrary is that of $B(OH)_4^-$ increases. This lead to the decreases ratio of $B(OH)_3$ to $B(OH)_4^-$, so the α_{d-sw} decreases. When pH reaches 12 (PZC of $Mg(OH)_2$), the adsorption quantity of $B(OH)_4^-$ decreases suddenly, and the relative ratio of $B(OH)_3$ to $B(OH)_4^-$ increases (Fig. 5), so the α_{d-fsw} also increases.

Our results indicate that $B(OH)_3$ is preferentially incorporated into the solid phase during the deposition of brucite. In a precipitated experiment of calcium carbonates from artificial seawater, Xiao et al. (2006) obtained the result that the boron isotopic

fractionation factors between calcium carbonates and seawaters were higher than 1. They reasoned that the presence of Mg^{2+} or other microelements was the main reasons of this observation and concluded that the heavier $B(OH)_3$ species was incorporated preferentially into $Mg(OH)_2$. The results of our study further confirmed the conclusion of Xiao et al. (2006).

4 Model of boron incorporated into brucite

Model 1: boron adsorption by minerals

The boron adsorption by minerals can be explained by phenomenological equation (Keren et al., 1981). It is supposed that when $B(OH)_3$, $B(OH)_4^-$ and OH^- coexist in solution, they can be adsorbed by $Mg(OH)_2$, metal oxides and clay minerals, and the affinity coefficients K_{B3} , K_{B4} and K_{OH} are $K_{B3} < K_{B4} < K_{OH}$ for $B(OH)_3$, $B(OH)_4^-$ and OH^- , respectively (Keren et al., 1981). They compete for the same adsorption site on solid. When pH is less than 7, $B(OH)_3$ is dominant. Because K_{B3} to clay mineral is very low, the boron adsorption is relatively minor. Under this pH value, the concentration of $B(OH)_4^-$ and OH^- is very low. Although they have relatively stronger affinity to clay, the contribution of them to the total boron adsorption is still very little. When pH increases to 9, $B(OH)_4^-$ concentration increases rapidly. Compared with $B(OH)_4^-$, OH^- concentration is still lower. So the adsorbed boron increases rapidly. When pH further increases, OH^- concentration will increase evidently, and the boron contribution decreases because of the competition for adsorption site with $B(OH)_4^-$.

In this study when pH is lower than 10, K_d increases as the pH increases (Fig. 2b). The K_d reaches its highest values at pH 10. When pH is higher than 10, K_d decreases and shows a mild trend after pH 12. The variation characteristics of K_d with pH can also be explained partly by this model. But isotopic fractionation characteristics of boron, the maximum adsorption value and K_d value of brucite deposit can not be explained by this totally.

Boron isotope fractionation during brucite deposition

J. Xiao et al.

Title Page

Abstract

Introduction

Conclusions

References

Tables

Figures

⏪

⏩

◀

▶

Back

Close

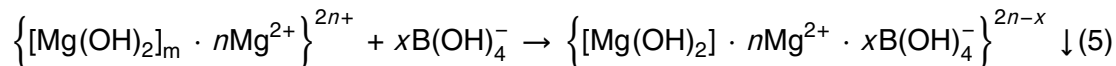
Full Screen / Esc

Printer-friendly Version

Interactive Discussion



The incorporation of $\text{B}(\text{OH})_4^-$ into brucite may be related with adsorption. Previous studies (Liu et al., 2004; Garcia-Soto and Camacho, 2006; Yuan et al., 2006) have indicated that the incorporation of boron into brucite or MgO was an adsorption process. When Mg^{2+} exists in solution, it can be adsorbed by brucite crystallite, and the resulting positive charge can adsorb the negatively charged $\text{B}(\text{OH})_4^-$. The equation is shown as follows:



If model 1 is applied, the $\delta^{11}\text{B}_{\text{d}}$ should be lower than $\delta^{11}\text{B}_{\text{isw}}$ and $\alpha_{\text{d-sw}}$ should be lower than 1. In this study, however, the results show that all $\delta^{11}\text{B}_{\text{d}}$ are higher than $\delta^{11}\text{B}_{\text{isw}}$ and $\alpha_{\text{d-sw}}$ values are higher than 1. This suggests that the model 1 is not suitable to explain all the data in our study.

The apparent pH dependence of the fractionation between carbonates and clays can be described in terms of the α_{3-4} and the pK_a of the boric acid-borate equilibrium (Sanchez-Valle et al., 2005). This model explains the B isotopic fractionation data for inorganically and biologically precipitated carbonates and clays, and suggests that in minerals like clay and other layered hydroxides, surface charge properties play an important role by changing the apparent acid-base equilibrium constant.

In our study, pK_a of the boric acid-borate equilibrium may be affected due to the presence of positive charge on the $\text{Mg}(\text{OH})_2$ surface. The fraction and $\delta^{11}\text{B}$ of boron species calculated using different pK_a versus pH values is shown in Fig. 6, which suggests that the influence of pK_a on fraction and $\delta^{11}\text{B}$ of boron species is big for solution with $\text{pH} < 10$. When $\text{pH} > 10$, the influence of pK_a is insignificant. For example, the $\delta^{11}\text{B}_{\text{isw3}}$ calculated using pK_a 7.0, 8.0 and 9.0 ($\alpha_{4/3} = 0.975$) are 16.08‰, 5.57‰ and -4.74‰, respectively for pH 8, and 18.44‰, 18.21‰ and 15.89‰, respectively for pH 10. When $\text{pH} > 11$, there are basically no differences among them. The pH values of our experiments are higher 10, so the isotopic fractionation characteristics of boron do not attributed to the change of pK_a .

Boron isotope fractionation during brucite deposition

J. Xiao et al.

Title Page

Abstract

Introduction

Conclusions

References

Tables

Figures

◀

▶

◀

▶

Back

Close

Full Screen / Esc

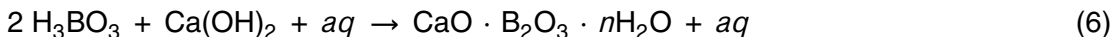
Printer-friendly Version

Interactive Discussion

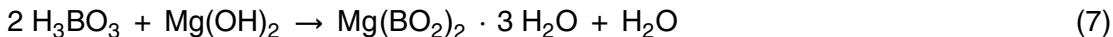


Model 2: chemical reaction of $B(OH)_3$ with $Mg(OH)_2$

Rodionov et al. (1991) reported that when limewater was added to seawater, $CaO \cdot B_2O_3 \cdot nH_2O$ was deposited. This reaction is shown as follows:



During deposition of brucite, a similar reaction may occur. $MgO \cdot B_2O_3 \cdot nH_2O$ may also be deposited. This hypothesis was confirmed by the XRD analyses of brucite. Compared with Fig. 7a, the brucite peak in Fig. 8 is clear, with apparent peaks of pinnoite ($Mg(BO_2)_2 \cdot 3H_2O$) and szaibelyite ($MgBO_2(OH)$). Judged from quantity and intensity of these peaks, pinnoite content should be higher than that of szaibelyite. As pH increases, the borate peak gradually weakens (Fig. 7b–g). When pH is 12.5 (Fig. 7g), its peak is very close to that of $Mg(OH)_2$, though the characteristic pinnoite peak is still observed. The pinnoite is the result of the following reaction between brucite and H_3BO_3 :



The above reaction cannot occur for $B(OH)_4^-$. So F_{d3} can exceed F_{fsw3} due to the preferential incorporation of H_3BO_3 into $Mg(OH)_2$, which enriches the deposited brucite in ^{11}B . The presence of szaibelyite may be the result of $B(OH)_4^-$ adsorption.

If model 2 is applied, the $\delta^{11}B_d$ should be higher than $\delta^{11}B_{fsw}$ and α_{d-sw} values should be higher than 1. Furthermore, $\delta^{11}B_d$ and α_{d-sw} should decrease with increasing pH values. In our study, all the $\delta^{11}B_d$ values are enriched in the heavy isotope compared relative to the $\delta^{11}B_{fsw}$ (Fig. 3a), and all the α_{d-fsw} are greater than 1 (Fig. 3b), which are consistent with model 2. But the α_{d-fsw} shows a wavy pattern (Fig. 3b), which indicates a complex isotopic fractionation process and can not be explained completely by model 2.

The fraction of boric acid in solution is negligible at high pH values (Fig. 1a), so that the $B(OH)_3$ incorporated into brucite should be little. But the F_{d3} is much higher than

CPD

7, 887–920, 2011

Boron isotope fractionation during brucite deposition

J. Xiao et al.

Title Page

Abstract

Introduction

Conclusions

References

Tables

Figures

⏪

⏩

◀

▶

Back

Close

Full Screen / Esc

Printer-friendly Version

Interactive Discussion



the $F_{\text{isw}3}$ (Fig. 5). This may be related with the transformation of borate to boric acid. After $\text{B}(\text{OH})_3$ is incorporated into brucite, $F_{\text{isw}3}$ decreases. In order to keep balance of $\text{B}(\text{OH})_3/\text{B}(\text{OH})_4^-$ ratio, $\text{B}(\text{OH})_4^-$ in solution would transform to $\text{B}(\text{OH})_3$. Meanwhile, the total boron quantity in solution decreases compared with initial solution. When a new equilibrium reaches, $\text{B}(\text{OH})_3$ continues to incorporate into brucite, and $\text{B}(\text{OH})_4^-$ in solution will transform to $\text{B}(\text{OH})_3$ to keep the equilibrium. This process will repeat, and finally the $F_{\text{d}3}$ is much higher than the $F_{\text{isw}3}$. But the total boron quantity in solution is much less than that in the initial solution.

Model 3: both chemical reaction and adsorption of boron incorporated into brucite

Many studies have indicated that only $\text{B}(\text{OH})_4^-$ is incorporated preferentially into marine carbonates (Vengosh et al., 1991; Hemming et al., 1992, 1995; Spivack et al., 1993; Sanyal et al., 1995, 1996, 1997, 2000). Under this circumstance, all the $\delta^{11}\text{B}$ values of carbonates are considered to be paralleled with the theoretical $\delta^{11}\text{B}_{\text{sw}3}$ and are lower than that of the parent seawater; $\alpha_{\text{carb-sw}}$ between carbonates and seawater are lower than 1 and increase with pH. When boron is adsorbed by oxides or clay minerals, the adsorption ability of $\text{B}(\text{OH})_4^-$ is much stronger than that of $\text{B}(\text{OH})_3$. The $\text{B}(\text{OH})_4^-$ is also incorporated preferentially into oxides or clay minerals, causing the enrichment of ^{10}B in oxides or clay minerals. Our results show that $\delta^{11}\text{B}_{\text{d}}$ is higher than $\delta^{11}\text{B}_{\text{isw}}$ and parallels neither with $\delta^{11}\text{B}_{\text{isw}4}$ nor with $\delta^{11}\text{B}_{\text{isw}3}$, but changes from decreases to increase with an inflexion at pH 12 (Fig. 3b). This indicates that both $\text{B}(\text{OH})_4^-$ and $\text{B}(\text{OH})_3$ are incorporated into brucite, and the latter is incorporated into brucite preferentially. Boron incorporation into brucite may be controlled by two processes: chemical reaction of $\text{B}(\text{OH})_3$ with brucite and $\text{B}(\text{OH})_4^-$ adsorption onto brucite. The simultaneous occurrence of these two processes decides the boron concentration and isotopic fractionation of brucite. The mechanisms of boron incorporated into brucite are distinct from those of carbonates and oxides or clay minerals.

Boron isotope fractionation during brucite deposition

J. Xiao et al.

[Title Page](#)[Abstract](#)[Introduction](#)[Conclusions](#)[References](#)[Tables](#)[Figures](#)[◀](#)[▶](#)[◀](#)[▶](#)[Back](#)[Close](#)[Full Screen / Esc](#)[Printer-friendly Version](#)[Interactive Discussion](#)

5 The influence of brucite on isotopic composition of boron in corals

Brucite exists in a wide range of common reef-building coral in Great Barrier Reef and Florida (Nothdurft et al., 2005). Fortunately, the brucite in older corals was lack due to being dissolved in seawater, where it is undersaturated (Nothdurft et al., 2005).

Inadvertent sampling of corals containing brucite could be responsible for anomalies Mg/Ca vs. SST plots in corals. Many studies have shown that $B(OH)_4^-$ is the dominant species incorporated into corals or foraminifers and ^{10}B enrich in corals (Vengosh et al., 1991; Hemming and Hanson, 1992; Spivack et al., 1993; Sanyal et al., 1995, 1996, 1997), but Klochko et al. (2009) found that both trigonal and tetrahedral coordinated boron existed in biogenic and hydrothermal carbonates. The occurrence of brucite in coral may change the isotopic composition of boron in coral due to the heavier $B(OH)_3$ species is incorporated preferentially into brucite and the deviant high boron isotopic composition of corals may associate with the occurrence of brucite. An exploratory study on the influence of brucite on the boron isotopic composition in modern corals is justifiable.

6 Conclusions

Based on the above experimental results, the following conclusions can be drawn:

1. Boron concentration of deposited brucite and partition coefficient K_d between deposited brucite and resultant seawater is controlled by pH of solution. The incorporation capacity of boron into brucite is much stronger than that into oxides and clay minerals.
2. All the $\delta^{11}B_d$ values are higher than $\delta^{11}B_{fsw}$ and all the fractionation factors α_{d-fsw} are higher than 1, indicating the preferential incorporation of H_3BO_3 into $Mg(OH)_2$. The mechanism of boron incorporated into brucite is distinct from that of carbonates deposition.

CPD

7, 887–920, 2011

Boron isotope fractionation during brucite deposition

J. Xiao et al.

Title Page

Abstract

Introduction

Conclusions

References

Tables

Figures

◀

▶

◀

▶

Back

Close

Full Screen / Esc

Printer-friendly Version

Interactive Discussion



Boron isotope fractionation during brucite deposition

J. Xiao et al.

Title Page

Abstract

Introduction

Conclusions

References

Tables

Figures

⏪

⏩

◀

▶

Back

Close

Full Screen / Esc

Printer-friendly Version

Interactive Discussion

3. During deposition of brucite, both H_3BO_3 and $\text{B}(\text{OH})_4^-$ incorporated into brucite. The simultaneous occurrences of boron adsorption onto brucite and precipitation reaction of H_3BO_3 with brucite decide the boron concentration and isotopic fractionation of the resulting brucite.

5 4. The isotopic compositions of boron in modern corals might be affected by both the existence of brucite in madrepora and the preferential incorporation of $\text{B}(\text{OH})_3$ into brucite. An exploratory study on the influence of brucite on the boron isotopic composition in modern corals is justifiable.

10 *Acknowledgements.* The authors thank Mr Guohong Gong, Bo Yang and Hua Ge for conducting the XRD and SEM analyses. This project was supported by the National Natural Science Foundation of China (Grant No. 40573013, 40776071 and 41003012), by innovation fund of Institute of Earth Environment, Chinese Academy of Sciences (Grant No. 0951071293).

References

15 Allison, N., Finch, A. A., and EIMF.: $\delta^{11}\text{B}$, Sr, Mg and B in a modern *Porites* coral: the relationship between calcification site pH and skeletal chemistry, *Geochim. Cosmochim. Acta*, 74, 1790–1800, 2010.

Catanzaro, E. J., Champion, C. E., Garner, E. L., Marinenko, G., Sappenfield, K. M., and Shield, W. R.: Boric acid: Isotopic and assay standard reference materials, *US Natl. Bur. Stand. Spec. Publ.*, 260–317 pp., 1970.

20 de la Fuente, M. M. and Muñoz, E.: Boron removal by adsorption with magnesium oxide, *Sep. Purif. Technol.*, 48, 36–44, 2006.

Fallon, S. J., McCulloch, M. T., Woesik, R., and Sinclair, D. J.: Corals at their latitudinal limits: Laser ablation trace element systematics in *Porites* from Shirigai Bay, Japan, *Earth. Planet. Sc. Lett.*, 172, 221–238, 1999.

25 Gaillardet, J. and Allègre, C. J.: Boron isotopic compositions of coral: Seawater or diagenesis record?, *Earth Planet. Sc. Lett.*, 136, 665–676, 1995.

Garcia-Soto, M. D. D. and Camacho, E. M.: Boron removal by means of adsorption with magnesium oxide, *Sep. Purif. Technol.*, 48, 36–44, 2006.

Boron isotope fractionation during brucite deposition

J. Xiao et al.

Title Page

Abstract

Introduction

Conclusions

References

Tables

Figures



Back

Close

Full Screen / Esc

Printer-friendly Version

Interactive Discussion



- Goldberg, S. and Glaubig, R. A.: Boron adsorption on aluminum and iron oxide minerals, *Soil Sci. Soc. Am. J.*, 49, 1374–1379, 1985.
- Goldberg, S. and Glaubig, R. A.: Boron adsorption and silicon release by the clay minerals kaolinite, montmorillonite, and illite, *Soil Sci. Soc. Am. J.*, 50, 1442–1446, 1986.
- 5 Hemming, N. G. and Hanson, G. N.: Boron isotopic composition and concentration in modern marine carbonates, *Geochim. Cosmochim. Acta*, 56, 537–543, 1992.
- Hemming, N. G., Reeder, R. J., and Hanson, G. N.: Mineral-fluid partitioning and isotopic fractionation of boron in synthetic calcium carbonate, *Geochim. Cosmochim. Acta*, 59, 371–379, 1995.
- 10 Hönisch, B. and Hemming, N. G.: Surface ocean pH response variations in $p\text{CO}_2$ two full glacial cycles, *Earth. Planet. Sc. Lett.*, 236, 305–314, 2005.
- Hönisch, B., Bickert, T., and Hemming, N. G.: Modern and Pleistocene boron isotope composition of the benthic foraminifer *Cibicides wuellerstorfi*, *Earth. Planet. Sc. Lett.*, 272, 309–318, 2008.
- 15 Ingri, N., Lagerström, G., Frydman, M., and Sillén, L. G.: Equilibrium studies of polyanions II polyborates in NaClO_4 medium, *Acta Chem. Scand.*, 11, 1034–1058, 1957.
- Keren, R. and Gast, R. G.: pH-dependent boron adsorption by montmorillonite hydroxy-aluminium complexes, *Soil Sci. Soc. Am. J.*, 47, 1116–1121, 1983.
- Keren, R., Gast, R. G., and Bar-Yosef, B.: pH-dependent boron adsorption by Namontmorillonite, *Soil Sci. Soc. Am. J.*, 45, 45–48, 1981.
- 20 Kingston, F. J., Posner, A. M., and Quirk, J. P.: Anion adsorption by goethite and gibbsite: 1. The role of the proton in determining adsorption envelopes, *J. Soil Sci.*, 23, 177–192, 1972.
- Klochko, K., Cody, G. D., Tossell, J. A., Dera, P., and Kaufman, A. J.: Re-evaluating boron speciation in biogenic calcite and aragonite using ^{11}B MAS NMR, *Geochim. Cosmochim. Acta*, 73, 1890–1900, 2009.
- 25 Lécuyer, C., Grandjean, P., Reynard, B., Albarède, F., and Telouk, P.: $^{11}\text{B}/^{10}\text{B}$ analysis of geological materials by ICP-MS Plasma 54: application to the boron fractionation between brachiopod calcite and seawater, *Chem. Geol.*, 186, 45–55, 2002.
- Lemarchand, E., Schott, J., and Gaillardet, J.: Boron isotope fractionation related to boron sorption on humic acid and the structure of surface complexes formed, *Geochim. Cosmochim. Acta*, 69, 3519–3533, 2005.
- 30

**Boron isotope
fractionation during
brucite deposition**

J. Xiao et al.

Title Page

Abstract

Introduction

Conclusions

References

Tables

Figures

◀

▶

◀

▶

Back

Close

Full Screen / Esc

Printer-friendly Version

Interactive Discussion



Lemarchand, E., Schott, J., and Gaillardet, J.: How surface complexes impact boron isotope fractionation: Evidence from Fe and Me oxide sorption experiments, *Earth Planet. Sc. Lett.*, 260, 277–296, 2007.

Liu, Y. S., Li, F. Q., and Wu, Z. M.: Study on adsorption of boron on magnesium hydroxide in brine, *J. Salt Lake*, 12, 45–48, 2004.

Marshall, J. F. and McCulloch, M. T.: An assessment of the Sr/Ca ratio in shallow water hermatypic corals as a proxy for sea surface temperature, *Geochim. Cosmochim. Acta*, 66, 3263–3280, 2002.

Mitsuguchi, T., Dang, P. X., Kitagawa, H., Uchida, T., and Shibata, Y.: Coral Sr/Ca and Mg/Ca records in Con Dao Island off the Mekong Delta: Assessment of their potential for monitoring ENSO and East Asian monsoon, *Global Planet. Change*, 63, 341–352, 2008.

Nothdurft, L. D., Webb, G. E., Buster, N. A., Holmes, C. W., Sorauf, J. E., and Kloprogge, J. T.: Brucite microbialites in living coral skeletons: Indicators of extreme microenvironments in shallow-marine settings, *Geology*, 33, 169–172, 2005.

Palmer, M. R. and Swihart, G. H.: Boron isotope geochemistry: an overview, *Rev. Mineral. Geochem.*, 33, 709–744, 1996.

Palmer, M. R., Spivack, A. J., and Edmond, J. M.: Temperature and pH controls over isotopic fractionation during absorption of boron marine clay, *Geochim. Cosmochim. Acta*, 51, 2319–2323, 1987.

Palmer, M. R., Pearson, P. N., and Cobb, S. J.: Reconstructing past ocean pH-depth profiles, *Science*, 282, 1468–1471, 1998.

Peak, D., Luther III, G. W., and Sparks, D. L.: ATR-FTIR spectroscopic studies of boric acid adsorption on hydrous ferric oxide, *Geochim. Cosmochim. Acta*, 67, 2551–2560, 2003.

Pearson, P. N. and Palmer, M. R.: Middle Eocene seawater pH and atmospheric carbon dioxide concentration, *Science*, 284, 1824–1826, 1999.

Pearson, P. N. and Palmer, M. R.: Atmospheric carbon dioxide concentrations over the past 60 million years, *Nature*, 406, 695–699, 2000.

Petric, N., Martinac, V., Labor, M., and Mirošević-Anzulović, M.: Isothermal and activated sintering of magnesium oxide from sea water, *Mater. Chem. Phys.*, 53, 83–87, 1998.

Pokrovsky, O. S. and Schott, J.: Experimental study of brucite dissolution and precipitation in aqueous solutions: surface speciation and chemical affinity control, *Geochim. Cosmochim. Acta*, 68, 31–45, 2004.

**Boron isotope
fractionation during
brucite deposition**

J. Xiao et al.

Title Page

Abstract

Introduction

Conclusions

References

Tables

Figures



Back

Close

Full Screen / Esc

Printer-friendly Version

Interactive Discussion



Pokrovsky, O. S., Schott, J., and Castillo, A.: Kinetics of brucite dissolution at 25°C in the presence of organic and inorganic ligands and divalent metals, *Geochim. Cosmochim. Acta*, 69, 905–918, 2005.

Rodionov, A. I., Voitova, O. M., and Romanov, N. Y.: The current state of the problem of the elimination of boron from waste waters, *Russ. Chem. Rev.*, 60, 1271–1279, 1991.

Sanchez-Valle, C., Reynard, B., Daniel, I., Lecuyer, C., Martinez, I., and Chervin, J. C.: Boron isotopic fractionation between minerals and fluids: New insights from in situ high pressure-high temperature vibrational spectroscopic data, *Geochim. Cosmochim. Acta*, 69, 4301–4313, 2005.

Sanyal, A., Hemming, N. G., Hanson, G. N., and Broecker, W. S.: Evidence for a high pH in the glacial ocean from boron isotopes in foraminifera, *Nature*, 373, 234–236, 1995.

Sanyal, A., Hemming, N. G., Broecker, W. S., Lea, D. W., Spero, H. J., and Hanson, G. N.: Oceanic pH control on the boron isotopic composition of foraminifera: evidence from culture experiments, *Paleoceanography*, 11, 513–517, 1996.

Sanyal, A., Hemming, N. G., Broecker, W. S., and Hanson, G. N.: Changes in pH in the eastern equatorial Pacific across stage 5–6 boundary based on boron isotopes in foraminifer, *Glob. Biogeochem. Cy.*, 11, 125–133, 1997.

Sanyal, A., Nugent, N., Reeder, R. J., and Bijma, J.: Seawater pH control on the boron isotopic composition of calcite: evidence from inorganic calcite precipitation experiments, *Geochim. Cosmochim. Acta*, 64, 1551–1555, 2000.

Smith, P. L. and Delong, R. C.: Brucite in modern corals, *Geol. Soc. Am. Abstracts with Programs*, p. 494, 1978.

Spivack, A. J., You, C. F., and Smith, H. J.: Foraminiferal boron isotopic ratios as a proxy for surface ocean pH over the past 21 Myr, *Nature*, 363, 149–151, 1993.

Vengosh, A., Kolodny, Y., Starinsky, A., Chivas, A. R., and McCulloch, M. T.: Coprecipitation and isotopic fractionation of boron in modern biogenic carbonates, *Geochim. Cosmochim. Acta*, 55, 2901–2910, 1991.

Wang, L. M.: Adsorption effect of magnesium hydroxide on boron in seawater, *Sea-Lake Salt Chem. Ind.*, 32, 5–7, 2003.

Wang, Q. Z., Xiao, Y. K., Wang, Y. H., Zhang, C. G., and Wei, H. Z.: Boron separation by the two-step ion-exchange for the isotopic measurement of boron, *Chin. J. Chem.*, 20, 45–50, 2002.

Boron isotope fractionation during brucite deposition

J. Xiao et al.

Title Page

Abstract

Introduction

Conclusions

References

Tables

Figures

◀

▶

◀

▶

Back

Close

Full Screen / Esc

Printer-friendly Version

Interactive Discussion



Watanabe, T., Winter, A., and Oba, T.: Seasonal changes in sea surface temperature and salinity during the Little Ice Age in the Caribbean Sea deduced from Mg/Ca and $^{18}\text{O}/^{16}\text{O}$ ratios in corals, *Mar. Geol.*, 173, 21–35, 2001.

5 Xiao, Y. K., Beary, E. S., and Fassett, J. D.: An improved method for the high precision isotopic measurement of boron by thermal ionization mass spectrometry, *Int. J. Mass Spectrom. Ion Proc.*, 85, 203–213, 1988.

Xiao, Y. K., Liao, B. Y., Liu, W. G., Xiao, Y., and Swihart, G. H.: Ion ex-change extraction of boron from aqueous fluids by Amberlite IRA 743 resin, *Chin. J. Chem.*, 21, 1073–1079, 2003.

10 Xiao, Y. K., Li, S. Z., Wei, H. Z., Sun, A. D., Zhou, W. J., and Liu, W. G.: An unusual isotopic fractionation of boron in synthetic calcium carbonate precipitated from seawater and saline water, *Sci. China Ser. B*, 36, 263–272, 2006.

Xu, L. and Ye, D. H.: Study on electrical property of $\text{Mg}(\text{OH})_2$ after boron adsorption, *Mar. Sci.*, 37, 12–13, 1997.

15 Yuan, J. J., Cui, R., and Zhang, Y.: Study on the adsorption of magnesium hydroxide to boron in seawater and the removal of boron in brine, *J. Salt Chem. Ind.*, 36, 1–6, 2006.

Zeebe, R. E.: Stable boron isotope fractionation between dissolved $\text{B}(\text{OH})_3$ and $\text{B}(\text{OH})_4^-$, *Geochim. Cosmochim. Acta*, 69, 2753–2766, 2005.

Boron isotope fractionation during brucite deposition

J. Xiao et al.

Title Page

Abstract

Introduction

Conclusions

References

Tables

Figures



Back

Close

Full Screen / Esc

Printer-friendly Version

Interactive Discussion



Table 1. Chemical composition of the magnesium-free artificial seawater.

Chemical composition	NaCl	CaCl ₂	NaHCO ₃	KCl	NaBr	H ₃ BO ₃	Na ₂ SiO ₃	Na ₂ Si ₄ O ₉	H ₃ PO ₄	Al ₂ Cl ₆	LiNO ₃
Concentration (g L ⁻¹)	26.7260	1.1530	0.1980	0.7210	0.0580	0.2612	0.0024	0.0015	0.0020	0.0130	0.0013

Boron isotope fractionation during brucite deposition

J. Xiao et al.

Table 2. Boron concentration (ppm) and partition coefficient K_d between brucite deposit and final seawater.

T_{repose}	pH	9.5	10.0	10.5	11.0	11.5	12.0	12.5	13.0
0 h	$[B]_{\text{fsw}}$	4.60	1.92	2.59	4.63	10.25	15.60	21.68	22.88
	$[B]_{\text{d}}$	901.47	937.79	844.50	625.75	657.96	289.91	273.57	250.12
	K_d	196.03	487.52	325.59	135.12	64.21	18.58	12.62	10.93
20 h	$[B]_{\text{fsw}}$	5.16	1.93	3.17	5.80	15.29	20.80	21.74	24.57
	$[B]_{\text{d}}$	1859.15	951.54	885.06	844.48	685.33	413.16	325.89	228.61
	K_d	360.62	494.20	278.98	145.71	44.83	19.87	14.99	9.31

$[B]_{\text{fsw}}$ and $[B]_{\text{d}}$ are the boron concentrations in final seawater and deposit, respectively.

Title Page

Abstract

Introduction

Conclusions

References

Tables

Figures

◀

▶

◀

▶

Back

Close

Full Screen / Esc

Printer-friendly Version

Interactive Discussion



Boron isotope fractionation during brucite deposition

J. Xiao et al.

Table 3. Isotopic fractionation of boron between deposited brucite and solution.

Repose time pH	0 h			20 h		
	$\delta^{11}\text{B}_d$ (‰)	$\delta^{11}\text{B}_{\text{fsw}}$ (‰)	$\alpha_{d-\text{fsw}}^b$	$\delta^{11}\text{B}_d$ (‰)	$\delta^{11}\text{B}_{\text{fsw}}$ (‰)	$\alpha_{d-\text{fsw}}^b$
9.5	$3.54 \pm 0.1(2)^a$	$-25.09 \pm 0.1(2)$	1.0294	31.27(1)	$-24.27(1)$	1.0569
10.0	$7.77 \pm 0.5(2)$	$-31.11 \pm 0.1(2)$	1.0401	8.57(1)	$-29.53(1)$	1.0393
10.5	$1.89 \pm 0.1(2)$	$-29.38 \pm 0.2(2)$	1.0322	$-1.20 \pm 0.3(2)$	$-31.85(1)$	1.0317
11.0	$2.61 \pm 0.1(2)$	$-27.33 \pm 0.5(2)$	1.0308	5.04(1)	$-29.87(1)$	1.0360
11.5	$2.21 \pm 0.3(3)$	$-27.38 \pm 0.5(3)$	1.0304	2.45(1)	$-18.15 \pm 0.5(2)$	1.0210
12.0	$8.67 \pm 0.1(2)$	$-11.23 \pm 0.3(2)$	1.0201	8.99(1)	$-8.55(1)$	1.0177
12.5	$17.53 \pm 0.1(2)$	$-12.86 \pm 0.6(2)$	1.0308	18.89(1)	$-14.92(1)$	1.0343
13.0	$27.84 \pm 0.2(3)$	$-8.58 \pm 0.7(2)$	1.0367	$28.26 \pm 0.4(2)$	$-10.63(1)$	1.0393

(a) The number in brackets indicate measurement times; (b) $\alpha_{d-\text{fsw}}$ is the isotopic fractionation factor of boron between deposit and final seawater, calculated as $\alpha_{d-\text{fsw}} = (1000 + \delta^{11}\text{B}_d)/(1000 + \delta^{11}\text{B}_{\text{fsw}})$.

Title Page

Abstract

Introduction

Conclusions

References

Tables

Figures

◀

▶

◀

▶

Back

Close

Full Screen / Esc

Printer-friendly Version

Interactive Discussion



Boron isotope fractionation during brucite deposition

J. Xiao et al.

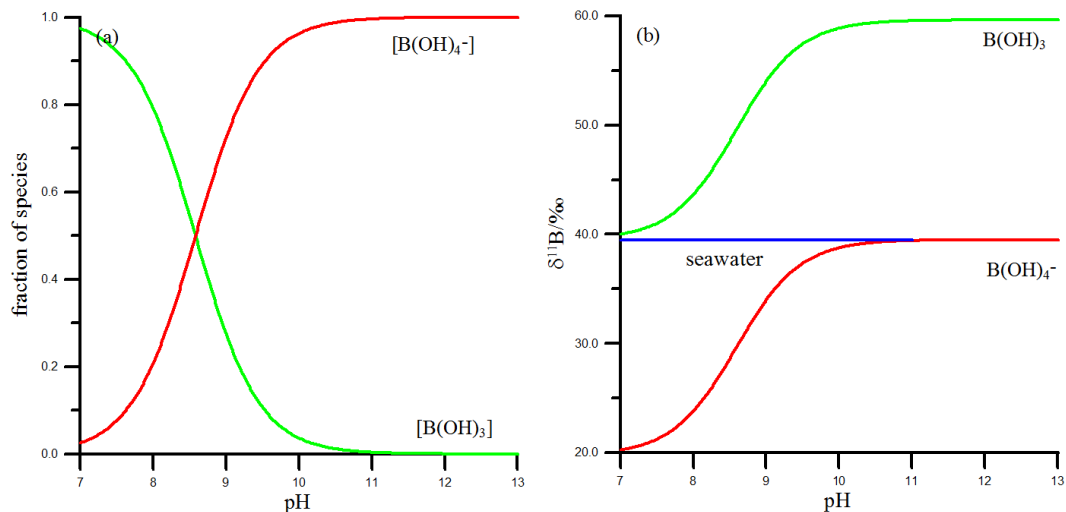


Fig. 1. Fraction (a) of the major dissolved boron species $B(OH)_3$ and $B(OH)_4^-$ in seawater and stable boron isotope fractionation (b) between them as a function of pH, using $pK_b = 8.58$ (Dickson, 1990).

Boron isotope fractionation during brucite deposition

J. Xiao et al.

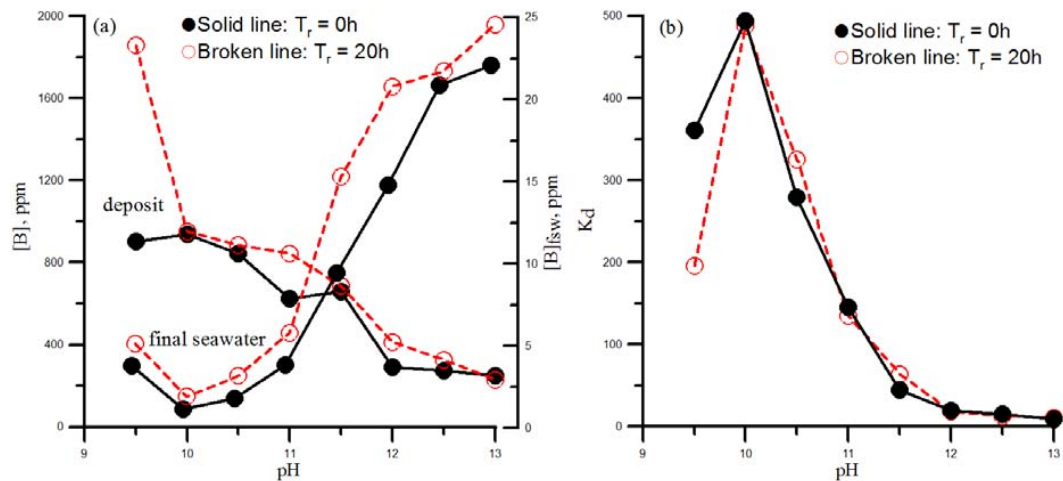


Fig. 2. Boron concentrations (a) and partition coefficients K_d (b) between brucite deposit and final seawater for $T_r = 0\text{ h}$ and 20 h .

Title Page

Abstract

Introduction

Conclusions

References

Tables

Figures

◀

▶

◀

▶

Back

Close

Full Screen / Esc

Printer-friendly Version

Interactive Discussion



Boron isotope fractionation during brucite deposition

J. Xiao et al.

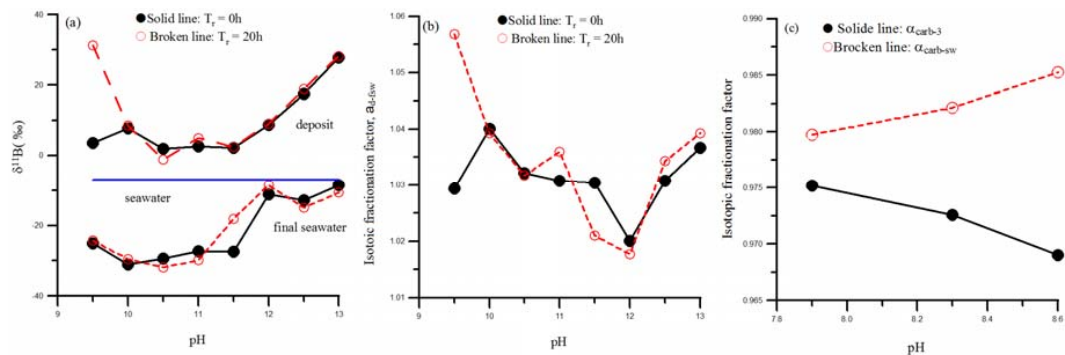


Fig. 3. Isotopic compositions (a) and fractionation factor (b) of boron between brucite deposit and solution for $T_r = 0\text{h}$ and 20h and (c) between inorganic carbonate and seawater (Sanyal et al., 1996).

Title Page

Abstract

Introduction

Conclusions

References

Tables

Figures

⏪

⏩

◀

▶

Back

Close

Full Screen / Esc

Printer-friendly Version

Interactive Discussion

Boron isotope fractionation during brucite deposition

J. Xiao et al.

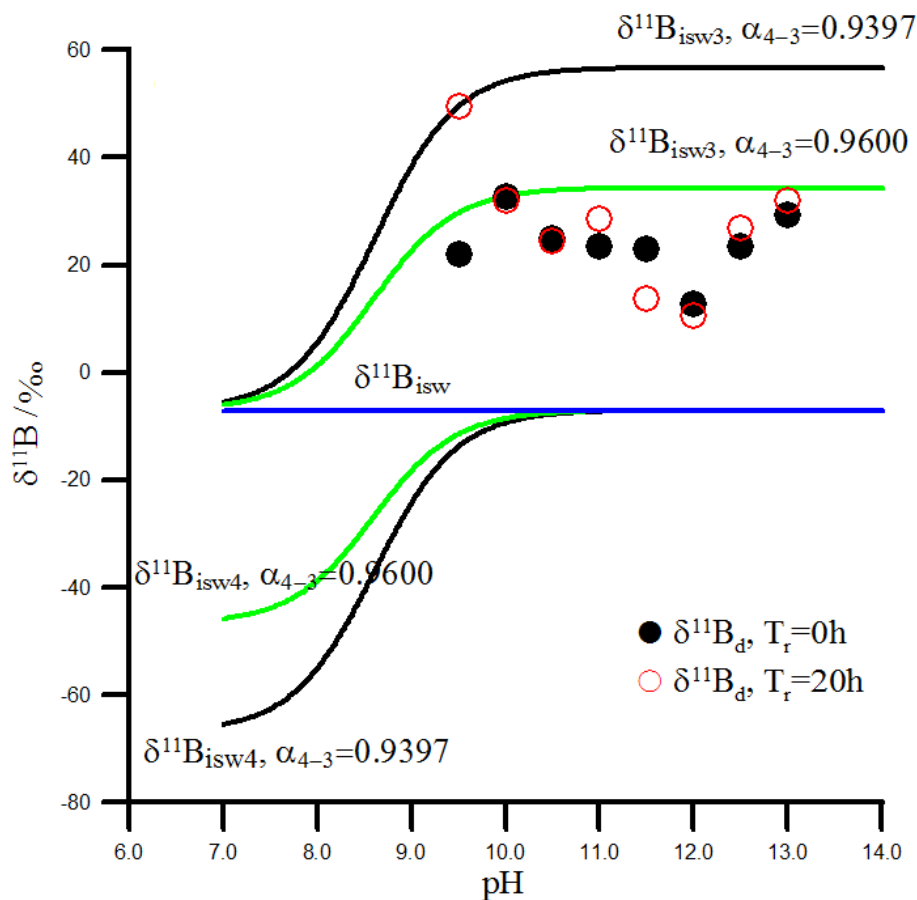


Fig. 4. $\delta^{11}\text{B}_d$ of brucite deposit and $\delta^{11}\text{B}_{\text{isw3}}$ and $\delta^{11}\text{B}_{\text{isw4}}$ of $\text{B}(\text{OH})_3$ and $\text{B}(\text{OH})_4^-$ in initial seawater calculated using different α_{4-3} versus pH values of parent solution.

Title Page

Abstract

Introduction

Conclusions

References

Tables

Figures

◀

▶

◀

▶

Back

Close

Full Screen / Esc

Printer-friendly Version

Interactive Discussion



Boron isotope fractionation during brucite deposition

J. Xiao et al.

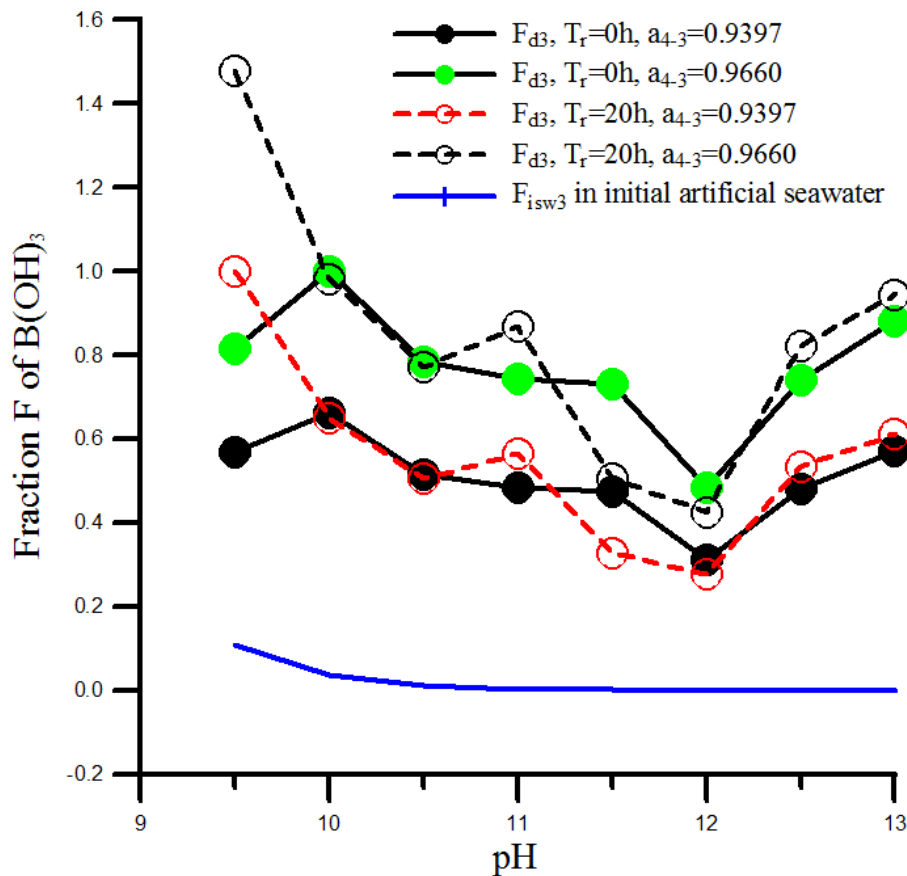


Fig. 5. Fraction F_{d3} of $B(OH)_3$ in brucite deposit calculated according to $\delta^{11}B_d$ with different α_{4-3} .

Title Page

Abstract

Introduction

Conclusions

References

Tables

Figures

◀

▶

◀

▶

Back

Close

Full Screen / Esc

Printer-friendly Version

Interactive Discussion



Boron isotope fractionation during brucite deposition

J. Xiao et al.

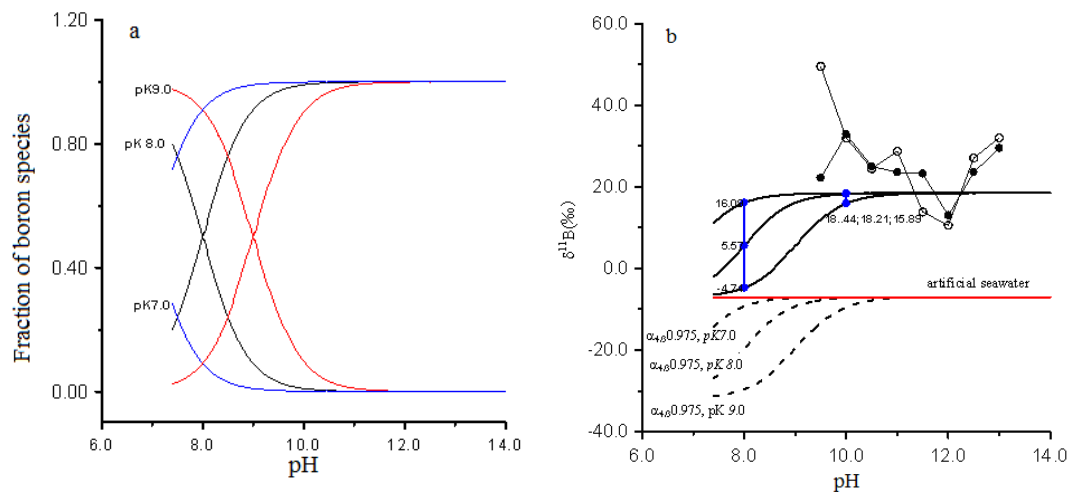


Fig. 6. The fraction (a) and $\delta^{11}B$ (b) of boron species calculated using different pK_a versus pH values.

Title Page

Abstract

Introduction

Conclusions

References

Tables

Figures

◀

▶

◀

▶

Back

Close

Full Screen / Esc

Printer-friendly Version

Interactive Discussion

**Boron isotope
fractionation during
brucite deposition**

J. Xiao et al.

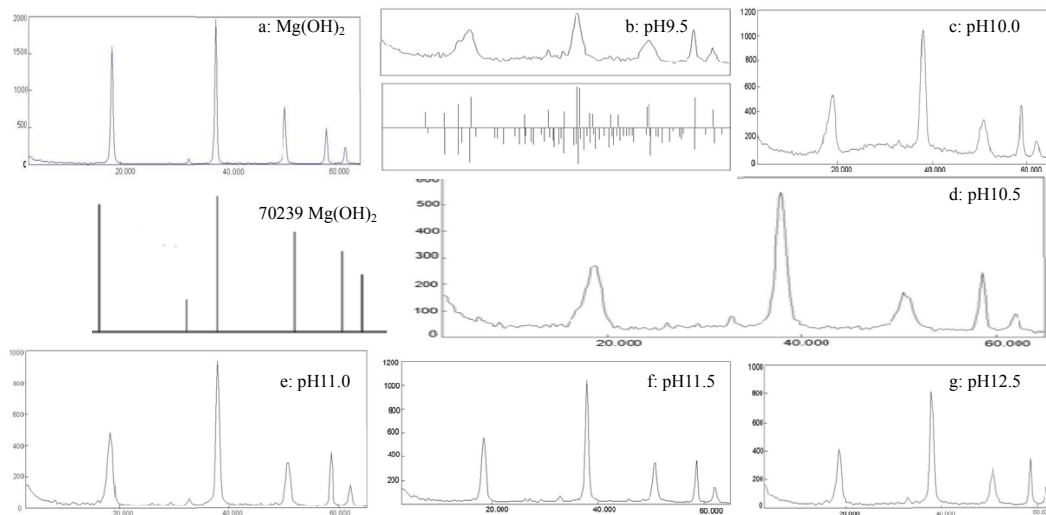


Fig. 7. X-Ray diffractogram of brucite deposited from artificial seawater at different pH values. **(a)** XRD of brucite from boron-free artificial seawater at pH 10.0, **(b–g)** XRD of brucite in our experiments.

[Title Page](#)[Abstract](#)[Introduction](#)[Conclusions](#)[References](#)[Tables](#)[Figures](#)[◀](#)[▶](#)[◀](#)[▶](#)[Back](#)[Close](#)[Full Screen / Esc](#)[Printer-friendly Version](#)[Interactive Discussion](#)

Boron isotope fractionation during brucite deposition

J. Xiao et al.

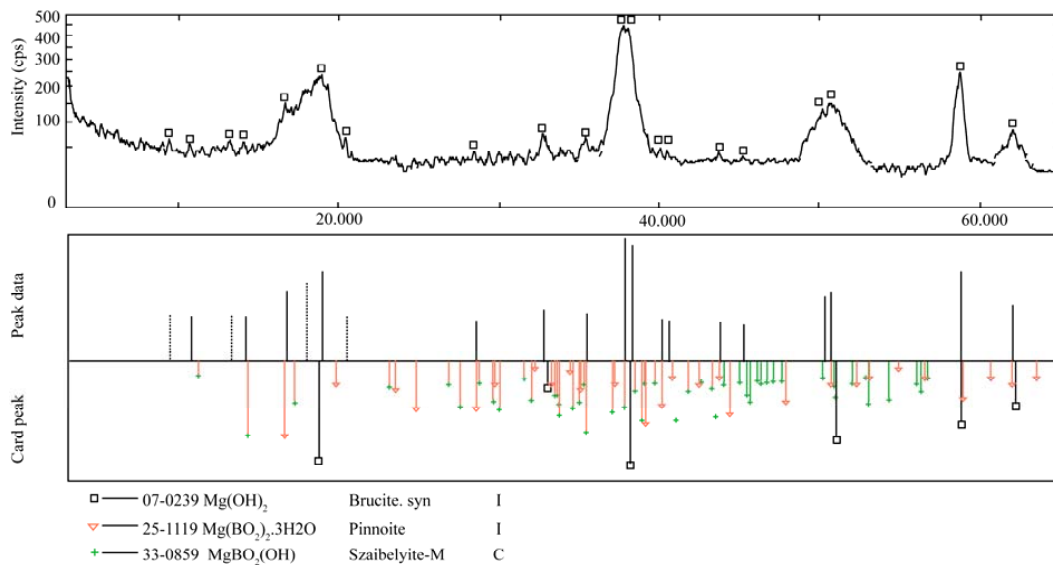


Fig. 8. X-Ray diffractogram of brucite deposited from B-containing artificial seawater at pH 9.5. It is a magnified figure of Fig. 6b.

Title Page

Abstract

Introduction

Conclusions

References

Tables

Figures

◀

▶

◀

▶

Back

Close

Full Screen / Esc

Printer-friendly Version

Interactive Discussion

